Surface electrochemistry of the oxidation of glycine at Pt

DANIEL G. MARANGONI, RICHARD S. SMITH, AND SHARON G. ROSCOE[1]
Chemistry Department, Acadia University, Wolfville, N.S., Canada B0P 1X0

Received September 21, 1988

DANIEL G. MARANGONI, RICHARD S. SMITH, and SHARON G. ROSCOE. Can. J. Chem. **67**, 921 (1989).

The electrochemical oxidation of glycine at a Pt electrode was investigated in aqueous solutions at pH 1 and 13 using steady-state current–potential measurements, cyclic voltammetry, and open circuit potential decay. The capacitance behaviour and the high Tafel slopes suggest the production of free radicals at the surface of the electrode accompanied by a second reaction involving loss of CO_2 which is the rate determining step. In the electro-oxidation of glycine, it appears that the adsorbed intermediate species is either hydrolyzed anodically to formaldehyde and ammonia, or is oxidized to a carbonium ion which is subsequently hydrolyzed to formaldehyde and ammonia in solution. This behaviour differs from the dimerization process typical of the radical reactions associated with the Kolbe mechanism.

Key words: glycine, amino acid, electrochemical oxidation, surface electrochemistry, Kolbe mechanism.

DANIEL G. MARANGONI, RICHARD S. SMITH et SHARON G. ROSCOE. Can. J. Chem. **67**, 921 (1989).

Faisant appel à des mesures de potentiel du courant à l'état stationnaire, à la voltamétrie cyclique et à la dégénérescence du potentiel en circuit ouvert et opérant en solutions aqueuses, à des pH de 1 et de 13, on a étudié l'oxydation électrochimique de la glycine, au niveau d'une électrode de Pt. Le comportement de la capacitance et les courbes de Tafel élevées suggèrent qu'il y a une production de radicaux libres à la surface de l'électrode et que celle-ci est accompagnée d'une deuxième réaction, impliquant une perte de CO_2, qui détermine la vitesse de la réaction. Dans l'électro-oxydation de la glycine, il semble que l'espèce intermédiaire adsorbée est soit hydrolysée à l'anode en formaldéhyde et en ammoniac soit oxydée en un carbocation qui est subséquemment hydrolysé en formaldéhyde et en ammoniac, en solution. Ce comportement diffère du processus de dimérisation typique des réactions radicaliques associées au mécanisme de la réaction de Kolbe.

Mots clés : glycine, acide aminé, oxydation électrochimique, électrochimie de surface, mécanisme de la réaction de Kolbe.
[Traduit par la revue]

Introduction

Several investigations of the electro-oxidation of α-amino acids were reported in the early 1930's (1–5). Fichter and Schmid (1) concluded from product analysis, that the electrolytic oxidation of α-amino acids in sulfuric acid solution produces the next lower aldehyde in the first step of the oxidation. However, Takayama (2, 3) found that oxidation at a PbO_2 anode resulted in a facile further oxidation of the aldehyde by the following:

$$RCH(NH_2)COOH \xrightarrow{[o]} RCHO + NH_3 + CO_2$$

$$RCHO \xrightarrow{[o]} RCOOH$$

Fichter and Kuhn (2) and Takayama (5) reported the formation of ammonia, formaldehyde, formic acid, carbon dioxide, and methyl, dimethyl, and trimethyl amines as products from the electrolytic oxidation of glycine. Plochl (6) has suggested that the amines probably resulted from the interaction of formaldehyde and ammonia. Takayama concluded that, from the experimental results, the first stage of the oxidation of amino acids is the aldehyde formation and that the other products either result from further oxidation (formation of carboxylic acids) or the chemical interaction of one product with another. He also concluded that the general reaction above best represents the course of the electrolytic oxidation of an α-amino acid.

The present research has been undertaken to investigate the kinetics, mechanisms, and surface effects of the electrochemical oxidation of glycine at the Pt electrode. Steady-state current–potential measurements, cyclic voltammetry, and open circuit potential decay have been used to study 0.45 *M* aqueous solutions of glycine at pH 1 and pH 13 in order to characterize these reactions with a fully protonated and fully unprotonated reactant, respectively. Anodic reactions in aqueous solutions at the Pt electrode are complicated by the electrocatalytic surface oxide film which develops on the anode metal surface. Thus, electrocatalysis occurs for such reactions as O_2 (7, 8), Cl_2 (9–13), N_2 (from N_3^-) (14–17) evolution, and the Kolbe reaction (18). Generally, in anodic reactions in aqueous media, the electrode may be considered "demetallized" (19) by its oxide film. Thus, the present work examines the influence of surface oxidation on the kinetics of anodic oxidation of glycine on well defined states of the Pt surface oxide film.

Experimental

(a) Methods

Steady-state polarization measurements were made on solutions of the amino acid at a pH of 1 and 13. A Wenking potentiostat (Fast Rise Model 6288RS) was used to control the potential of the working electrode, and the current and potential measurements were read from Keithley autoranging multimeters (model 175 and model 195), respectively. Polarization lines were determined by holding for 10 s per current-density point, at 10 mV intervals of potential. Data analysis and graphics were carried out using both the Cyber 830 and Commodore PC-10 computers.

Corrections for uncompensated solution resistance ("*iR*" drop corrections) were made to the Tafel plots. These "*iR*" corrections were determined using a mercury-wetted vacuum relay to give a clean fast break in the circuit, and the rapid potential drop was recorded on a digital storage Tektronics oscilloscope (model 5440). Potential decay transients were determined in the same manner following steady-state potentiostatic polarization. Analysis of the potential–time data was accomplished using a Commodore PC-10 computer with the Asystant data processing software.

Cyclic voltammograms were obtained using the potentiostat and a function generator (Hokuto Denko Ltd, Model HB-111) to produce a repeating triangular potential function. The potential, read directly from the working and the reference electrodes, and the current, measured by the potential across a variable resistor placed in the counter electrode circuit, were connected to a Hewlett-Packard X-Y recorder (model HP 489-5093) to give the potential–current profile.

[1]To whom correspondence should be addressed.

(b) Solutions

Solutions of glycine were prepared from 99+% purity, gold label reagent (Aldrich Chemical Company) using conductivity water (Nanopure water, resistivity = 18.3 megohm cm^{-1}) which had been distilled from acid potassium permanganate to remove organic impurities. Sulfuric acid solutions were prepared from Aristar grade 98% purity reagent (BDH Chemicals Limited), while sodium hydroxide solutions were prepared from the standardized Aldrich Acculute concentrate. All solutions were prepared to a concentration of 0.45 *M* in amino acid.

(c) Electrochemical cell and electrodes

Three compartment, all glass cells, provided with glass-sleeved stopcocks as two of the compartments, were used. A specially designed gas-tight cell having a small volume was used for analysis of electrogenerated gaseous products by means of gas chromatography. Johnson Matthey and Mallory high-purity grade Pt wires were degreased by refluxing in acetone, sealed in soft glass, and electrochemically cleaned by potential cycling in 1 *M* sulfuric acid, and stored in 98% H_2SO_4. The reference electrodes used were saturated calomel electrodes made according to a standard procedure (19). Their potentials were checked frequently against a standard hydrogen electrode and compared with the literature value (20). The saturated calomel electrodes were found to be reproducible to within ±1 mV.

(d) Product analysis

A Perkin-Elmer model 226 gas chromatograph fitted with a flame ionization detector was used to detect products from electrolysed solutions of glycine at pH 1 and pH 13. The 2.5 m by 0.6 cm copper column, packed with Chromosorb 103, was maintained at 140°C. This column packing is selective for nitrogen-containing compounds, aldehydes, and some lower molecular weight alcohols. In addition, formaldehyde was quantitatively determined from electrolysed solutions of glycine maintained at carefully controlled anodic potentials, using the pentane-2,4-dione colorimetric method (21). Carbon dioxide was detected by passing the evolved gases through a saturated BaOH solution. Ammonia was determined by the Kjeldahl method (22).

Results

Tafel plots derived from the steady-state polarization experiments for each of the systems studied are shown in Figs. 1 and 2, and the numerical values for the Tafel slopes determined by least-squares analysis are presented in Table 1. The Tafel slopes for both systems are significantly higher than those normally observed for oxygen evolution in aqueous solution (i.e. $2.3(2RT/F) = 120$ mV) (23). In Fig. 2, the Tafel plots for the amino acid under acidic conditions (pH 1) showed a long linear Tafel region with a slope which was twice those observed for oxygen evolution. In a 1 *M* sulfuric acid solution, in the absence of amino acid, oxygen evolution occurs at 1.36 V, E_{SCE}. This difference in the Tafel behaviour may be attributed to the barrier layer effect observed by Conway and Dzeiciuch (24) where the oxygen evolution reaction is suppressed because of a dipole barrier due to the presence of adsorbed species on the surface of the electrode.

A different effect is observed under alkaline conditions. There is a distinct inflection observed in the Tafel slopes (Fig. 1). This is similar to that observed in the Kolbe reaction of acetate ion in aqueous solution (18) and again appears at the same potential where oxygen evolution would occur in a 1 *M* sodium hydroxide solution (i.e. 1.10 V, E_{SCE}). Thus it appears, as in the Kolbe mechanism, that the oxygen evolution reaction is suppressed by the amino acid anion. Glycine shows an unusually high Tafel slope over this potential region. The value of 363 mV corresponds to a Tafel slope of $3(2.3(2RT/F))$. It is also interesting that below the inflection region the slope is the same as those observed under acidic conditions.

Cyclic voltammograms for glycine in both alkaline and acidic solutions are shown in Figs. 3 and 4. Table 2 shows the numerical values for the charge Q_0 associated with the formation of oxide, the charge Q_r due to the reduction of the surface oxide, and the ratio Q_0/Q_r. A comparison may also be made of the charge from the oxidation process with that of the reduction process in a sulfuric acid or sodium hydroxide solution.

The results from Table 2 show that the charge Q_r due to the reduction of the oxide is very much smaller than Q_0 in all cases, suggesting that there are species other than the normal oxide adsorbed on the surface of the electrode which are not removed during the oxide reduction process. The ratio of Q_r for oxide reduction to Q_r (=210 μC cm^{-2}) for hydrogen reduction is also significant. For a sulfuric acid solution in the absence of amino acids this ratio is about 2.5 (18). For amino acids at pH 1, the ratio is about 2.1, whereas an even smaller ratio of ca. 1.0 is observed in solutions of pH 13. This indicates that adsorption by amino acids occurs at platinum causing a reduction in the

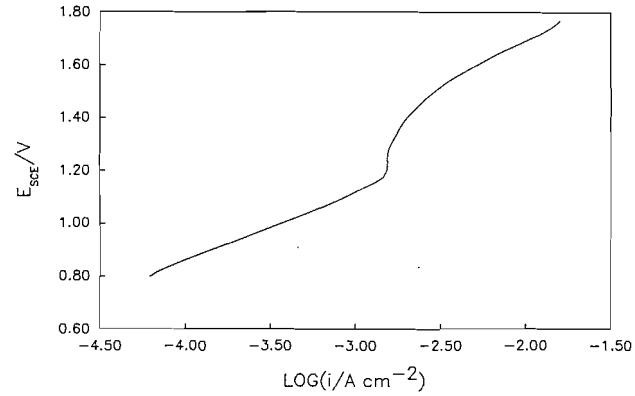

FIG. 1. Tafel behaviour of 0.45 *M* glycine in NaOH (pH 13) at the Pt electrode.

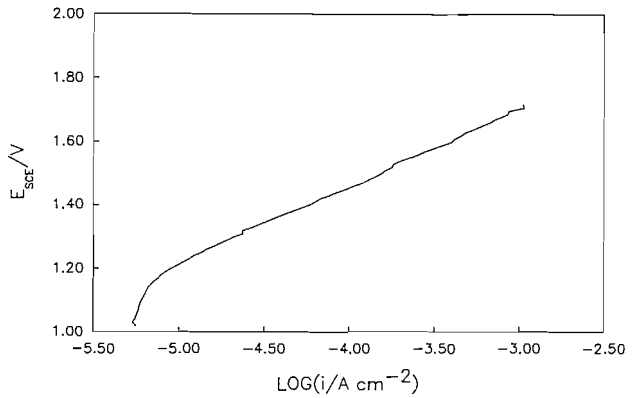

FIG. 2. Tafel behaviour of 0.45 *M* glycine in H_2SO_4 (pH 1) at the Pt electrode.

TABLE 1. Experimental Tafel parameters for the electro-oxidation of glycine (0.45 *M*) in acidic and alkaline solutions

pH	Potential range (E_{SCE} (V))	Tafel slope *b* (mV)
13.0	(0.900–1.100)	239
13.0	(1.480–1.700)	363
1.0	(1.280–1.680)	237

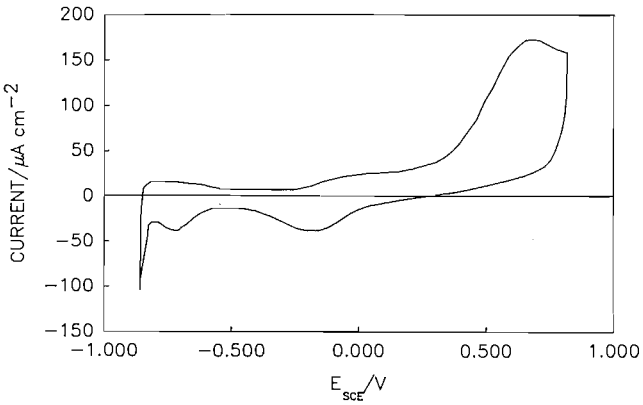

FIG. 3. Cyclic-voltammogram of 0.45 *M* glycine in NaOH (pH 13) at the Pt electrode.

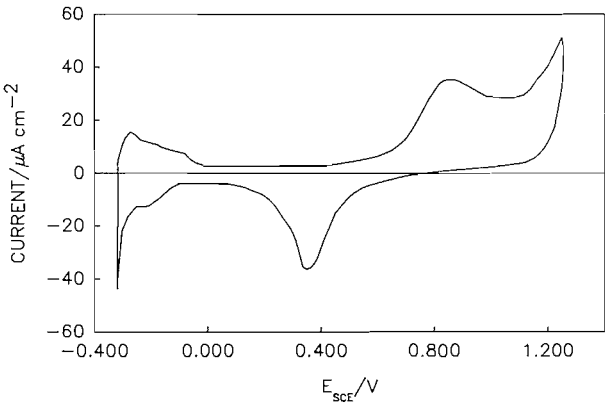

FIG. 4. Cyclic-voltammogram of 0.45 *M* glycine in H_2SO_4 (pH 1) at the Pt electrode.

TABLE 2. Evaluation of the charge and surface coverage of the cyclic voltammograms of glycine (0.45 *M*) at a platinum electrode

pH	Potential range (E_{SCE} (V))	Q_0 ($\mu C\,cm^{-2}$)	Q_r ($\mu C\,cm^{-2}$)	Q_0/Q_r
13.0	(−0.854–0.816)	2136	223	9.58
1.0	(−0.317–1.220)	1315	451	2.92

normal oxide growth due to a blocking effect by the bulkier molecules with an even stronger adsorption and diminished oxide formation occurring in the basic solutions. This is also consistent with the larger Q_0/Q_r for anodic oxidation and reduction in the basic compared with the acidic solutions. In the aqueous acid solution (Fig. 4) a blocking effect by glycine of the submonolayer film of upd (underpotential deposition) OH species occurs similar to the blocking effect of Cl^- ions adsorbed at Pt electrodes during anodic Cl_2 evolution from an aqueous solution (25–29).

Open circuit potential decay curves for glycine in basic and acidic solutions are shown in Figs. 5 and 7. Plots of potential versus log $(-dV/dt)$ were obtained from a curve-fitting routine on the potential versus time data. Multiple correlation coefficients were determined using the *F*-test. In all cases, the fit was better than 99.99%. The pseudo-capacitance (C_ϕ) was then evaluated as a function of potential (Figs. 6 and 8) (30).

These graphs indicate a rapid decrease in capacitance in the basic solution at the lower potentials to a capacitance of about

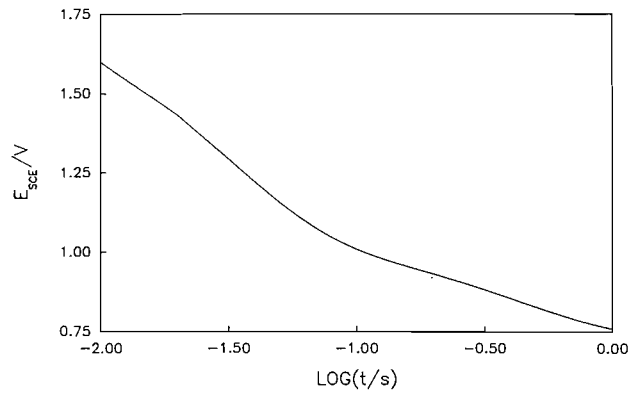

FIG. 5. Open-circuit potential decay of 0.45 *M* glycine (pH 13) at the Pt electrode.

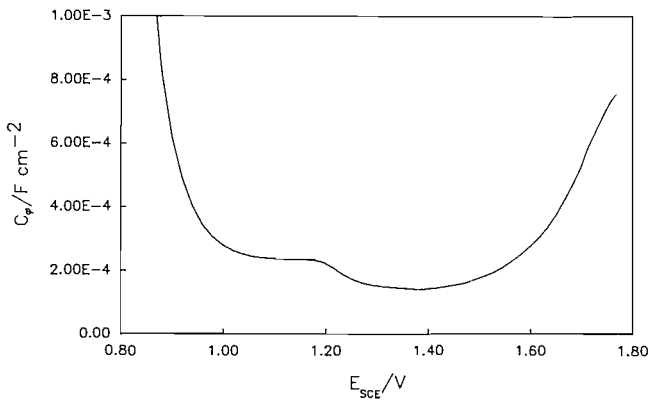

FIG. 6. Capacitance behaviour at anodic potentials of 0.45 *M* glycine (pH 13) at the Pt electrode.

250 $\mu F\,cm^{-2}$ (Fig. 5). An inflection in the capacitance is observed at potentials coincident with the inflection in the Tafel plot (Fig. 1). The capacitance decreases to a minimum of about 100 $\mu F\,cm^{-2}$ before increasing again at higher potentials, indicating that the initial coverage of adsorbed species on the electrode surface is rapidly diminished as the Faradaic process proceeds. This decrease in surface coverage corresponds to a mechanism where the initial or electron discharge step is slow, followed by fast consecutive reactions which reduce the surface coverage (31). The inflection regions in the capacitance and the Tafel plots suggest a change in the mechanism of the reaction associated with surface coverage of adsorbed species.

The potential decay curve in the acidic solution shows three linear regions with very small changes in slope (Fig. 7). These correspond to very slight inflections observed in the Tafel slope (Fig. 2). However, the plots of C_ϕ versus potential (Fig. 8) show a similar rapid decrease in capacitance followed by an increase to ca. 600 $\mu F\,cm^{-2}$ at a potential of 1.47 V. This behaviour is similar to the inflection region observed in the alkaline solution.

Qualitative analysis of the products obtained from the electrolysis of glycine agreed with those found by Fichter and co-workers (1, 2) and Takayama (3–5). The electrolysis was carried out at high current densities under controlled potentials of 2.2 V in the acidic solution and 1.8 V in the basic solution. The products identified by gas chromatographic analysis were formaldehyde and methyl and trimethyl amine in acidic solution and formaldehyde and methyl amine in the basic solution. Carbon dioxide and ammonia were also detected as products of the electrolysis. A quantitative analysis of the formaldehyde

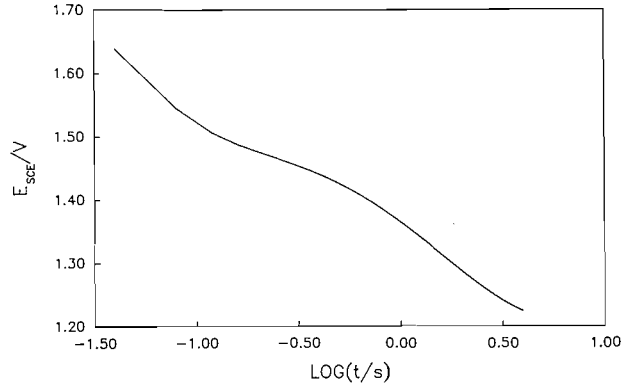

FIG. 7. Open-circuit potential decay of 0.45 *M* glycine (pH 1) at the Pt electrode.

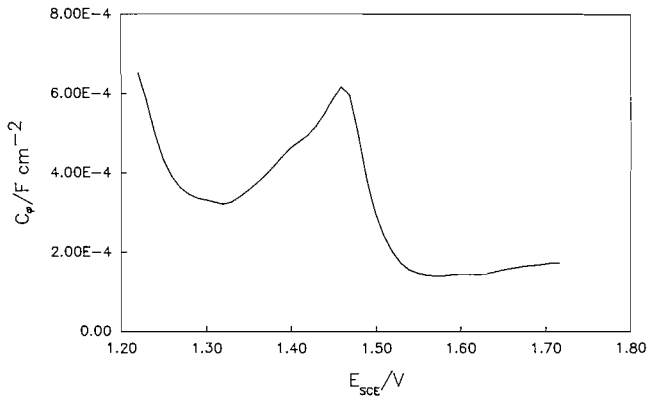

FIG. 8. Capacitance behaviour at anodic potentials of 0.45 *M* glycine (pH 1) at the Pt electrode.

formed after electrolyzing the basic solution at an anodic potential of 1.32 V, E_{SCE} using the pentane-2,4-dione colorimetric method (21) indicated an 85–90% yield. From the same experiments, analysis of ammonia using the Kjeldahl method (22) indicated ca. 83% yield. When the electrolysis was carried out at the anodic potential of 1.06 V, E_{SCE}, which is just below the inflection region, the yield of formaldehyde dropped to 60% and ammonia to ca. 55%.

Discussion

Analysis of the products of the electro-oxidation of glycine shows that formaldehyde is the main product in both basic and acidic conditions. Ammonia and carbon dioxide were also detected as products of this reaction in agreement with Fichter (1, 2). These products suggest a dissociative, adsorptive type of mechanism, with the overall reaction for the basic solution

$$CH_2(NH_2)COO^- + OH^- \rightarrow CH_2O + NH_3 + CO_2 + 2e$$

The thermodynamic potential for the basic glycine solution was calculated to be 1.33 V, E_{SCE} using the standard free energies of formation (20). A similar calculation for the acidic solution gave a value of 1.17 V, E_{SCE}. These correspond to the observed inflection regions discussed previously which are also coincident with the potentials for oxygen evolution, which suggests that oxygen evolution is suppressed by the amino acid oxidation process in a manner similar to that observed for the Kolbe reaction (24). The overall reaction must, however, be written in terms of elementary electrochemical steps because it has become well established in electrodics that it is not energetically favourable for two electrons to tunnel simultaneously between the solution and the metal surface (32). Elementary steps using single electron transfer are therefore preferred.

TABLE 3. Theoretical Tafel slopes calculated on the basis of each of the steps being rate-determining for the mechanism proposed for the electro-oxidation of glycine at Pt

RDS	Theoretical Tafel slope	Calculated Tafel slope (mV)	r_2/r_1
Step I	$2.3(2RT/F)$	120	—
Step II	$2.3(2RT/F)(r_1/(r_1 - r_2))$	180	0.33
		240	0.50
		360	0.66
Step III	$2.3(2RT/F)(r_1/(r_1 + r_2))$	90	0.33
		80	0.50
		72	0.66

The production of CO_2 in the alkaline solution may be explained by a series of steps similar to the initial two steps in the Kolbe reaction (18),

$$CH_2(NH_2)COO^- \rightarrow CH_2(NH_2)COO(M) + e$$
$$CH_2(NH_2)COO(M) \rightarrow NH_2CH_2(M) + CO_2$$

This series of steps could lead to formaldehyde and ammonia by either of two routes, a hydrolysis reaction of the adsorbed radical accompanied by an electron transfer at the surface of the electrode,

$$NH_2CH_2(M) + OH^- \rightarrow NH_3 + CH_2O + e$$

or with the formation of a carbonium ion by electron transfer (18, 33) followed by subsequent hydrolysis in solution to give ammonia and formaldehyde:

$$NH_2CH_2(M) \rightarrow NH_2CH_2^+ + e$$
$$NH_2CH_2^+ + OH^- \rightarrow NH_3 + CH_2O$$

The corresponding mechanism for the acidic solution would be

$$CH_2(NH_3^+)COOH \rightarrow CH_2(NH_3^+)COO(M) + H^+ + e$$
$$CH_2(NH_3^+)COO(M) \rightarrow (NH_3^+)CH_2(M) + CO_2$$

followed by:

$$(NH_3^+)CH_2(M) + H_2O \rightarrow NH_4^+ + CH_2O + H^+ + e$$

A carbonium ion mechanism in the acidic solution, however, is rather unlikely due to the formation of a positive charge on adjacent atoms:

$$(NH_3^+)CH_2(M) \rightarrow (NH_3^+)CH_2^+ + e$$
$$(NH_3^+)CH_2^+ + H_2O \rightarrow NH_4^+ + CH_2O + H^+$$

In order to verify these mechanisms it is necessary to compare the experimentally determined Tafel slopes with those derived from theoretical considerations (34–36). The Tafel slope is calculated separately for each possible rate determining step (Table 3).

Considering step I of the mechanisms to be rate determining, the following rate expression is obtained:

$$i_1 = zFk_1(1 - \theta_{G\cdot})C_{G+}\exp\{-(\Delta G_1^{\neq} - \beta VF + \beta r_1\theta)/RT\}$$

where the subscript G· refers to the radical species on the electrode surface, G+ the amino acid species in the bulk solution, θ the fractional surface coverage, and β the symmetry factor, which will be considered for these calculations to be equal to

0.5, which is the value expected for most reactions (18). The possibility of very low values for β due to a barrier-layer discharge process will be discussed later. The r term is introduced in the above equation to allow for variation in the heat of adsorption with coverage.

The experimental Tafel slopes may be compared with those calculated from the rate expressions. For the case where step I is rate controlling the derivative is:

$$dV/d \log i_1 = 2.3(2RT/F)$$

If step II of the mechanisms were rate determining, the rate equation would rearrange as follows:

$$\ln i_2 = \ln zFk_2 + \ln (1 - \theta_{G1\cdot}) + \ln \theta_{G\cdot} - (\Delta G_2^{\neq} - \beta r_1\theta + (1 - \beta)r_2\theta)/RT$$

where G· refers to the initially adsorbed radical in step I and G_1· refers to the adsorbed radical after rearrangement occurs. Now if step II was rate controlling and step I was in quasi-equilibrium, and with β = 0.5, the equation may be written as

$$\ln i_2 = \ln zFk_2 + \ln (1 - \theta_{G1\cdot}) + \ln (\theta_{G\cdot}) - [\Delta G_2^{\neq} + (VF/2r_1)(r_2 - r_1)]/RT$$

Rearranging and differentiating gives

$$dV/d \ln i_2 = (2RT/F)[r_1/(r_1 - r_2)]$$

If step III of the mechanisms were rate determining

$$\ln i_3 = \ln zFk_3 + \ln \theta_{G1\cdot} - (\Delta G_3^{\neq} - \beta VF - \beta r_2\theta)/RT$$

Substituting in terms of θ and differentiating gives

$$dV/d \ln i_3 = (2RT/F)[r_1/(r_1 + r_2)]$$

The Tafel slopes obtained have factors designated as r related to the heats of adsorption. Under Temkin conditions, that is conditions of intermediate coverage, the r values become important, whereas under Langmuir conditions, either $\theta \cong 0$ or $\theta \cong 1$, these effects need not be considered. Under Temkin conditions, values must be assigned to r_1 and r_2. The high Tafel slopes may be explained by taking r_1 to be 1.5 to 2 times greater than r_2, and the Tafel slopes calculated in this way for each of the possible steps considered to be rate controlling are given in Table 3. From these results and a comparison with the Tafel slopes observed experimentally (Table 1), a mechanism consistent with step II as the rate-determining step is proposed.

For the alkaline solution of glycine, the experimental Tafel slope was 239 mV over the potential range 0.90 to 1.10 V, which is below the inflection region. This would correspond to $r_2/r_1 = 0.5$ where r_1 and r_2 represent the heats of adsorption of $CH_2(NH_2)COO^{\cdot}$ and $NH_2CH_2^{\cdot}$, respectively. At the inflection point, the Tafel slope increased abruptly to 363 mV which would correspond to $r_2/r_1 = 0.66$. The capacitance decreased abruptly at this point indicating a smaller surface coverage. At very high potentials the capacitance gradually increased due to the growth of thicker films of adsorbed species.

In the acidic solution of glycine, the Tafel slope of 237 mV again corresponds to a value of $r_2/r_1 = 0.5$ where r_1 and r_2 are now $CH_2(NH_3^+)COO^{\cdot}$ and $(NH_3^+)CH_2^{\cdot}$. An inflection region is not observed in the Tafel slope, although the capacitance behaviour shows an increase in surface coverage which maximizes and then drops as in the alkaline solution.

Similar Tafel relationships were obtained for the reaction of formate ion in 100% formic acid (36) and trifluoroacetate in 100% trifluoroacetic acid (24). The reaction mechanisms were treated in terms of a Temkin isotherm. In the case of the trifluoroacetate reaction, the value of r_1 for adsorption of the bulky polar $CF_3COO^{\cdot}$ was considered to be greater than that for the smaller $CF_3^{\cdot}$ groups.

If the mechanism involving formation of carbonium ions for step III proceeds as follows,

$$NH_2CH_2(M) \rightarrow NH_2CH_2^+ + e$$

followed by hydrolysis in solution to give ammonia and formaldehyde, a similar analysis for this step III as the rate-determining step results in the same theoretical Tafel slope as that obtained previously for step III (Table 3). Thus, although the mechanism may proceed via a carbonium ion intermediate formed in solution, it is not the rate-determining step for the process.

Another possibility which may be considered is the formation of the carbonium ion during the decarboxylation step, step II, although generally carbonium ion formation is considered to occur in a step following decarboxylation (18, 33).

$$CH_2(NH_2)COO(M) \rightarrow CO_2 + NH_2CH_2^+ + e$$

However, if this were the rate-determining step, the derivative would be

$$dV/d \log i_1 = 2.3(RT/2\beta F)$$

which gives a value of 60 mV for the Tafel slope if β = 0.5, which is too low a value compared to that observed experimentally.

High Tafel slopes observed in anodic oxidations of this type have also been interpreted by a change in the effective symmetry factor due to the formation of a thin moderately conducting dipole barrier-layer film of adsorbed species on the electrode (18, 24, 36). This may cause the effective symmetry factor to be less than 0.5. In order to explain the high Tafel slopes observed, the β values would have to be as low as 0.25 and 0.17 for the lower and upper Tafel slopes, respectively. However, there is evidence for strong adsorption of species as shown by the blocking of the upd OH species and the large anodic charge in the cyclic voltammograms. The capacitance behaviour shows a rapid decrease in surface coverage with increasing potential at the onset of the Faradaic process, which gives further evidence for the second step following adsorption being the rate determining step, followed by fast consecutive reactions (31). As even higher potentials are reached, the capacitance again begins to increase due to the strongly adsorbed intermediate species on the surface of the electrode. Therefore, although a barrier-layer film and consequently a modified β value may be used to explain the high Tafel slopes, there is evidence that a changing surface coverage due to adsorbed species may account for these results. It is of interest that a more normal vaue of β is actually observed for the acetate Kolbe reaction in completely anhydrous solution (18). Recently, the results of several studies of the Kolbe electrosynthesis under a variety of conditions have been attributed to the surface adsorption of radicals (37–39).

In conclusion, the mechanism of electrolytic oxidation of glycine at a platinum electrode, in both basic and acidic solution, may be accounted for by a radical mechanism for the first two steps similar to that observed for the Kolbe reaction with the loss of carbon dioxide, the second step in the mechanism being rate-determining. However, rather than the dimerization typical of those radical reactions associated with the Kolbe mechanism, it appears that the adsorbed intermediate species is either hydrolyzed anodically in these aqueous solutions to formaldehyde and ammonia, or is possibly further

oxidized to a carbonium ion which is subsequently hydrolyzed to ammonia and formaldehyde in solution.

1. F. FICHTER and M. SCHMID. Helv. Chim. Acta, **3**, 704 (1920).
2. F. FICHTER and F. KUHN. Helv. Chim. Acta, **7**, 164 (1924).
3. Y. TAKAYAMA. Bull. Chem. Soc. Jpn. **12**, 342 (1924).
4. Y. TAKAYAMA. Bull. Chem. Soc. Jpn. **8**, 213 (1933).
5. Y. TAKAYAMA. Bull. Chem. Soc. Jpn. **12**, 338 (1937).
6. PLOCHE. Ber. **21**, 2117 (1888).
7. D. DAMJANOVIC. *In* Modern aspects of electrochemistry. Vol. 5. *Edited by* J. O'M. Bockris and B. E. Conway. Plenum, New York. 1969. p. 369.
8. A. DAMJANOVIC, L. S. R. YEH, and J. F. WOLF. J. Electrochem. Soc. **127**, 784 (1980); **127**, 1951 (1980); **122**, 471 (1975).
9. E. L. LITTAUER and L. L. SHRIER. Electrochim. Acta, **11**, 527 (1966).
10. B. E. CONWAY and D. M. NOVAK. J. Chem. Soc. Faraday Trans. I, **75**, 2454 (1979).
11. B. E. CONWAY and D. M. NOVAK. J. Electroanal. Chem. **99**, 133 (1979).
12. B. E. CONWAY and J. MOZOTA. J. Chem. Soc. Faraday Trans. I, **78**, 1717 (1982).
13. S. G. ROSCOE and B. E. CONWAY. J. Electroanal. Chem. **224**, 163 (1987).
14. H. P. STOUT. Trans. Faraday Soc. **41**, 64 (1945).
15. L. KRISHTALIK and G. E. TITOVA. Elektrokhimiya, **4**, 285 (1968).
16. S. G. ROSCOE and B. E. CONWAY. J. Chem. Soc. Chem. Commun. 900 (1988).
17. S. G. ROSCOE and B. E. CONWAY. J. Electroanal. Chem. **249**, 217 (1988).
18. A. K. VIJH and B. E. CONWAY. Chem. Rev. **67**, 623 (1967).
19. Polariter Instructions Manual, Radiometer Company.
20. R. C. WEAST (*Editor*). CRC handbook of chemistry and physics. 64th ed. The Chemical Rubber Company, Cleveland. 1983.
21. S. C. CHURMS (*Editor*). CRC handbook of chromatography, carbohydrates. Vol. I. CRC Press, Inc., FL. 1982. p. 182.
22. I. M. KOLTOFF and E. B. SANDELL. Textbook of quantitative inorganic analysis. 3rd ed. MacMillan Co., New York. 1963. p. 538.
23. M. TARASEVICH, A. SADKOWSKI, and E. YEAGER. *In* Comprehensive treatise on electrochemistry. *Edited by* B. E. Conway *et al.* Plenum Press, New York. 1983. pp. 301–397.
24. B. E. CONWAY and M. DZIECIUCH. Can. J. Chem. **41**, 38 (1963).
25. A. K. N. REDDY, M. A. GENSHAW, and J. O'M. BOCKRIS. J. CHEM. PHYS. **48**, 671 (1968).
26. J. L. ORD and F. C. HO. J. Electrochem. Soc. **118**, 46 (1971).
27. R. PARSONS and W. VISSCHER. J. Electroanal. Chem. **36**, 329 (1972).
28. J. W. SCHULTZE and K. J. VETTER. J. Electroanal. Chem. **34**, 131, 141 (1972).
29. D. M. NOVAK and B. E. CONWAY. J. Chem. Soc. Faraday Trans. I, **77**, 2341 (1981).
30. B. E. CONWAY, L. BAI, and D. F. TESSIER. J. Electroanal. Chem. **161**, 39 (1984).
31. B. V. TILAK, C. G. RADER, and B. E. CONWAY. Electrochem. Acta, **22**, 1167 (1976).
32. J. O'M. BOCKRIS and A. K. N. REDDY. Modern electrochemistry. 1st ed. Vol. 2, Plenum Press. 1970. p. 1082.
33. J. H. P. UTLEY. *In* Techniques of electroorganic synthesis, Part I. *Edited by* N. L. Weinberg. Wiley, New York. 1974, pp. 793–906.
34. B. E. CONWAY and P. L. BOURGAULT. Can. J. Chem. **37**, 292 (1959).
35. J. O'M. BOCKRIS. J. Chem. Phys. **24**, 817 (1956).
36. B. E. CONWAY and M. DZIECIUCH. Can. J. Chem. **41**, 21 (1963).
37. Y. B. VASSILIEV, V. S. BAGOTZKY, E. P. KOVSMAN, V. A. GRINBERG, L. S. KANEVSKY, and V. R. POLISHCHYUK. Electrochem. Acta, **27**, 919 (1982).
38. R. M. CERVINO, W. E. TRIACA, and A. J. ARVIA. J. Electroanal. Chem. **172**, 255 (1984).
39. B. KRAEUTLER, C. D. JAEGER, and A. J. BARD. J. Am. Chem. Soc. **100**, 4903, 1978.